THE JOURNAL OF PHYSICAL CHEMISTRY C

Article

pubs.acs.org/JPCC

# Molecular-Scale Study of Salicylate Adsorption and Competition with Catechol at Goethite/Aqueous Solution Interface

Yanli Yang,[†] Jinming Duan,[‡] and Chuanyong Jing*[,†]

[†]State Key Laboratory of Environmental Chemistry and Ecotoxicology, Research Center for Eco-Environmental Sciences, Chinese Academy of Sciences, Beijing 100085, China

[‡]School of Environmental and Municipal Engineering, Xi'an University of Architecture and Technology, Xi'an 710055, China

Supporting Information

**ABSTRACT:** Insights into the adsorption mechanisms of salicylate on goethite, especially its competition with catechol, can further our understanding of the fate and transport of natural organic matter analogues in the environment. The adsorption process was investigated using multiple complementary techniques including batch adsorption experiments, flow-cell ATR-FTIR measurement, and DFT calculations. The macroscopic results show that increasing pH and ionic strength had an adverse effect on salicylate adsorption because of electrostatic interactions. Salicylate formed an inner-sphere complex in a mononuclear monodentate configuration with carboxylate bound to the iron atom on goethite surface within pH 5−9. The electrostatic outer-sphere complex could be observed under high salicylate concentrations and low ionic strength. In the competitive adsorption of salicylate and catechol, their individual interfacial complexes coexisted and competed with each other. The surface salicylate could be replaced by catechol during adsorption under neutral and basic pH conditions. Accordingly, the macroscopic adsorption capacity of salicylate was depressed in the binary system.

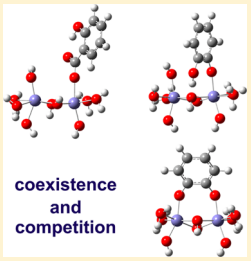


## INTRODUCTION

Salicylic acid is an important chemical in the environment due to its natural formation as well as its universal use as the pharmaceutical and additive in cosmetics and foodstuff.[1,2] Because of the existence of carboxylic and phenolic hydroxyl (ph-OH) groups in its structure, salicylic acid has been used as an analogue for natural organic matter (NOM) to explore the mechanisms of mineral−NOM interactions.[3−5] Moreover, the natural environment is a multicomponent system, and the importance of competitive adsorption with coexisting molecules cannot be overstated.[6]

The adsorption of salicylate on metal oxides has been extensively studied, but no consistent conclusion is obtained in its interfacial molecular structure. For example, salicylate adsorption on goethite was described as a mononuclear bidentate (M-B) complex involving a carboxylate ($COO^-$) oxygen, an ortho phenolic oxygen, and a surface iron atom.[3,4,7] In addition, Yost et al. proposed another interfacial configuration in an electrostatic outer-sphere complex or a binuclear bidentate (B-B) complex.[3] The controversial salicylate surface structures were also reported on $TiO_2$ surfaces. Some researchers suggest the M-B structure on $TiO_2$ involved both ph−OH and $COO^-$ groups.[8,9] Meanwhile, the B-B complexes were hypothesized by Janković et al.[10] Upon salicylate adsorption on aluminum (hydr)oxides, surface configurations such as mononuclear mondentate (M-M),[5,11,12] M-B,[9] and B-B[5,12] were proposed. The inconsistency in the proposed surface complex motivated our research in molecular-scale understanding of salicylate adsorption.

Extensive research has focused on the competitive adsorption between carboxylate and phosphate (sulfate),[2,13] two carboxylates,[6,14] as well as carboxylate and metal ions.[15,16] However, limited knowledge is available for competition mechanisms between carboxylate and phenolic aromatic compounds,[17] especially on the microscopic level. The functional groups determine, in a large extent, the adsorption behaviors of the compounds. Furthermore, insights from the dynamic adsorption process are crucial in determining the effects of functional groups on the interfacial configurations and adsorption affinity. Therefore, the adsorption process of salicylate was investigated in this study in the presence of catechol, a naturally occurring compound with two ph−OH groups. Goethite was selected as the model mineral due to its widespread occurrence in terrestrial soils and sediment.[18,19] The configurations of catechol on goethite are in M-M and B-B structures, and its dynamic adsorption process has been reported in our previous study.[20]

The objective of this study was to explore the interfacial configurations of salicylate on goethite under the effect of pH, concentration, ionic strength, and the competition with catechol. Multiple complementary techniques including bulk adsorption experiments, in situ flow-cell measurements of attenuated total reflectance Fourier-transform infrared (ATR-FTIR) spectroscopy, and quantum chemical calculations were used to study the adsorption mechanisms. The results should further our fundamental understanding on the interactions of NOM with iron oxide surfaces.

**Received:** March 20, 2013
**Revised:** April 27, 2013
**Published:** April 29, 2013

   dx.doi.org/10.1021/jp4027578 | J. Phys. Chem. C 2013, 117, 10597−10606

## EXPERIMENTAL SECTION

**1. Materials.** Salicylic acid and catechol were purchased from Sigma-Aldrich. All chemicals were of analytical reagent or higher and were used without further purification. The samples were prepared in Milli-Q water (18.2 MΩ), which was boiled for 60 min and cooled with nitrogen purging to remove $CO_2$. Goethite was synthesized and characterized, as shown in our previous work, with a point of zero charge (PZC) of 8.9 and a BET surface area of 84.7 $m^2/g$.[20]

**2. Macroscopic Adsorption Experiments.** The pH edge adsorption experiments of 1 mM salicylate on 5 g/L goethite were conducted in the presence and absence of 1 mM catechol as a function of solution pH. Suspension samples in 0.01 and 0.1 M NaCl were adjusted to desired pH values with NaOH and HCl. The adsorption isotherms of salicylate, catechol, and their binary competition were investigated at pH 7 in 0.1 M NaCl solution. The goethite concentration was fixed at 5 g/L, and the adsorbate concentration was increased up to 10 mM. After mixing on an end-over-end rotator for 12 h in the dark, samples were centrifuged and passed through a 0.22 μm membrane filter for analysis.

Salicylate and catechol concentrations were measured using a high-performance liquid chromatography (HPLC, Shimadzu LC-20A, Japan) with UV−visible detector at 284 nm. Analytical separations were carried out with a Hypersil Gold C18 column (150 mm × 4.6 mm i.d., particle size 5 μm, Thermo Fisher Scientific Inc.). A mobile phase of citric buffer (20 mM, pH 3.5)/methanol (80:20, v/v) was used.

**3. ATR-FTIR Spectroscopy Study.** The ATR-FTIR spectra were obtained using a Nicolet 6700 instrument equipped with a liquid-nitrogen-cooled MCT detector, a liquid pump (LC-3A, Shimadzu, Japan), and a 45° ZnSe crystal mounted in a flow cell (PIKE Technologies, USA). Spectra were collected using 256 scans at 4 $cm^{-1}$ resolution. Data acquisition and analysis, that is, subtraction, normalization, and baseline correction, were carried out using OMNIC software (Thermo Fisher Scientific, USA). The second derivative was used to justify the numbers and positions of the peak. A Gaussian line shape was employed in the curve-fitting analysis in the wavenumber ranges 1510−1420 and 1300−1180 $cm^{-1}$.[20,21]

The goethite film was coated on the ATR crystal following our previous report.[20] In brief, 400 μL of 1 g/L goethite suspensions was spread on the surface of the crystal and dried in an oven at 50 °C for 1 h. The crystal was gently rinsed with Milli-Q water before use. In the single adsorbate system, salicylate at concentrations of 1, 5, and 10 mM was analyzed in 0.01 and 0.1 M NaCl solution. In the direct competition system, solutions containing 1 mM salicylate and catechol in 0.1 M NaCl were passed through the flow cell at the rate of 0.4 mL/min. The dynamic process was also investigated by flowing single adsorbate for ∼65 min and then with competing molecules. The background spectrum was collected, and then the solution was changed to the sample with the same pH and NaCl concentration. Spectra were recorded as a function of time for 4 h.

**4. Quantum Chemical Calculations.** Calculations of geometry optimization and IR frequencies were performed using the Gaussian 09 program[22] with B3LYP hybrid density function theory (DFT). The frequency calculations were carried out with 6-31G +(d,p) basis set on the C, H, and O atoms (scale factor = 0.9642), coupled to a LanL2DZ basis set on the Fe atoms (scale factor = 0.9612).[23] The edge-sharing dioctahedral cluster was used to predict the optimized geometries and vibrational frequencies of salicylate on goethite surfaces.[21,24,25] Six explicit $H_2O$ molecules were added and combined with IEFPCM to consider the solvation effect.[25−27]

## RESULTS AND DISCUSSION

**1. Macroscopic Adsorption Studies.** The pH-dependent adsorption of salicylate on goethite in 0.01 and 0.1 M NaCl was in stark contrast with the adsorption of catechol (Figure 1).[20] Similar to typical anion adsorption behaviors,[28] the adsorption of salicylate decreased with increasing pH. The electrostatic attraction between the positively charged goethite surface (pH <8.9, PZC) and salicylate monoanion ($pK_{a1}$ = 2.97, $pK_{a2}$ = 13.7) may contribute to the adsorption.[28] Meanwhile, the surface coverage was significantly decreased with elevated ionic strength especially under acidic conditions (Figure 1A),

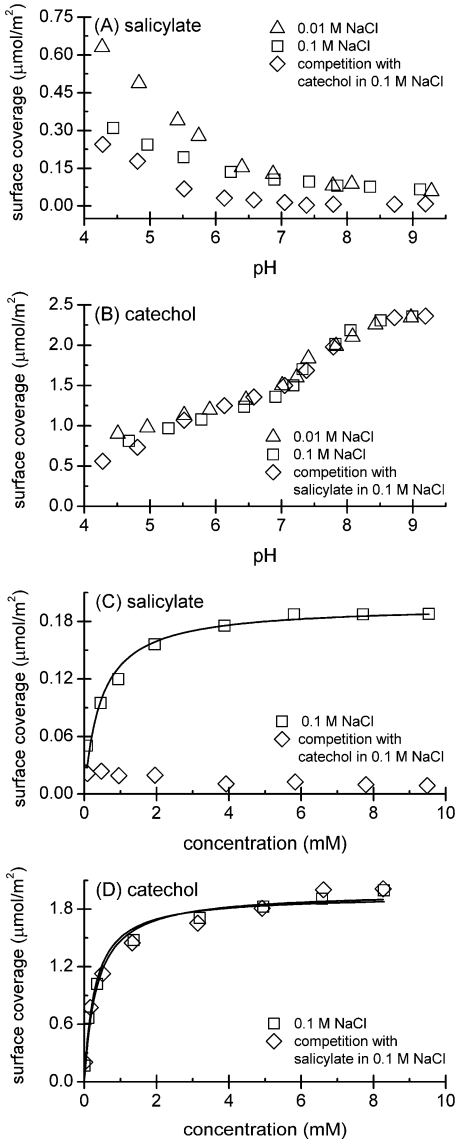


**Figure 1.** (A,B) pH-dependent adsorption edges of single salicylate and catechol, as well as competition with each other on goethite. (C,D) Adsorption isotherms of salicylate and catechol in the single and competition systems at pH 7. Symbols represent the experimental data points. Solid lines are Langmuir adsorption model simulations. pH edges of single catechol adsorption are from our previous study.[20]


dx.doi.org/10.1021/jp4027578 | J. Phys. Chem. C 2013, 117, 10597−10606

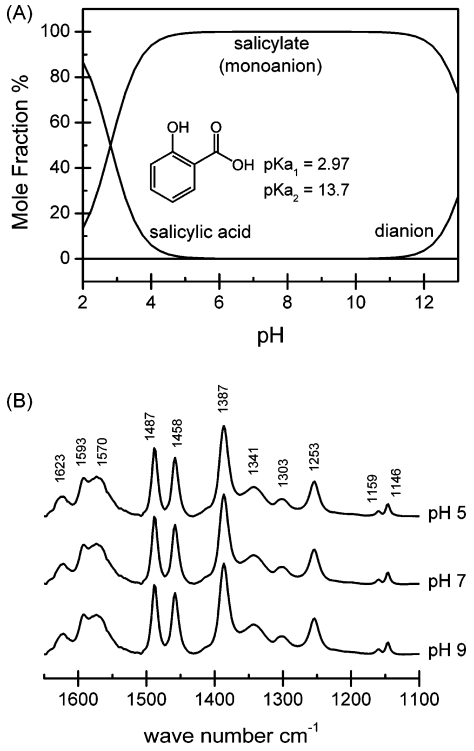


**Figure 2.** (A) Distribution of salicylic acid, salicylate (monoanion), and dianion as a function of pH in 0.1 M NaCl solution. (B) Spectra of the soluble salicylate (10 mM) at pH 5, 7, and 9 in 0.1 M NaCl solution.

**Table 1. Experimental and Calculated Peak Positions and Assignments for Salicylate (Monoanion)[a]**

| pH 5 | pH 7 | pH 9 | cal. | assignment |
|---|---|---|---|---|
| 1146 | 1146 | 1146 | 1118 | $\delta$(CH) |
| 1159 | 1160 | 1159 | 1130 | $\delta$(CH) |
| 1253 | 1253 | 1253 | 1231 | $\nu$(ph−OH) |
| 1303 | 1303 | 1303 | 1293 | $\nu$(CC) |
| 1341 | 1342 | 1341 | 1306 | $\nu_s$(COO−) |
| 1387 | 1387 | 1387 | 1398 | $\delta$(ph−OH), $\nu$(CC) |
| 1458 | 1458 | 1458 | 1436 | $\nu$(CC) |
| 1487 | 1487 | 1487 | 1471 | $\nu$(CC) |
| 1570 | 1570 | 1570 | 1555 | $\nu_{as}$(COO−) |
| 1593 | 1592 | 1593 | 1574 | $\nu$(CC) |
| 1623 | 1622 | 1622 | 1616 | $\nu$(CC) |

[a]Cal. refers to calculated frequencies for the salicylate (monoanion). Peak assignments are based on theoretical calculations.

indicating the existence of electrostatic outer-sphere surface complexes. Catechol, however, showed preferential adsorption on goethite under basic conditions (Figure 1B).[20] In addition, catechol (0.7 to 2.4 $\mu$mol/m$^2$) exhibited a higher adsorption capacity than salicylate (0.06 to 0.6 $\mu$mol/m$^2$) over pH range 4.3−9.3. In the presence of equal molar of salicylate and catechol (1 mM), the adsorption capacity of salicylate was suppressed by ∼20% under acidic condition and up to 90% under basic condition. However, no detectable difference in catechol adsorption was observed between single and binary systems.

To further compare their adsorption affinities, we conducted the adsorption isotherms of salicylate and catechol. In the single adsorbate system, the surface coverage of salicylate and catechol

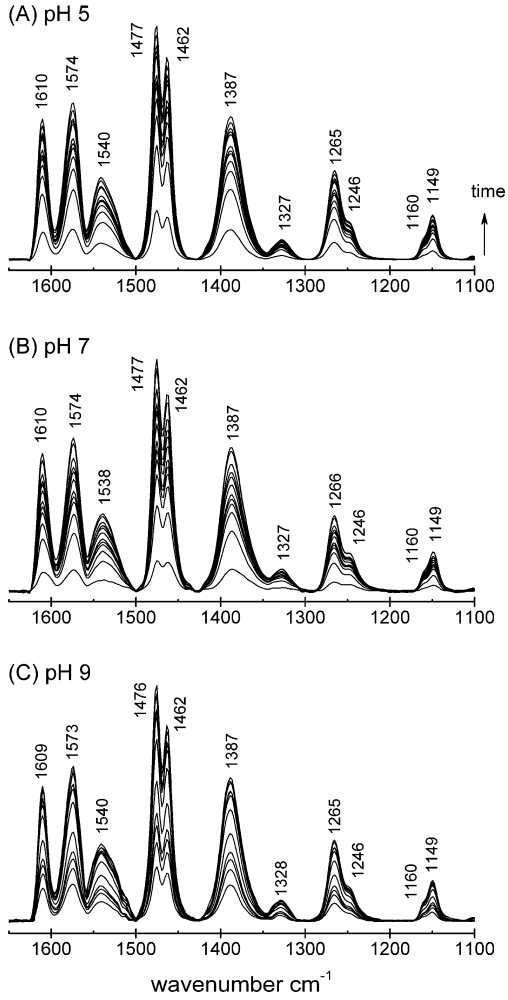


**Figure 3.** Time-dependent spectra of adsorbed species acquired at pH 5 (A), 7 (B), and 9 (C) with 1 mM salicylate in 0.1 M NaCl solution.

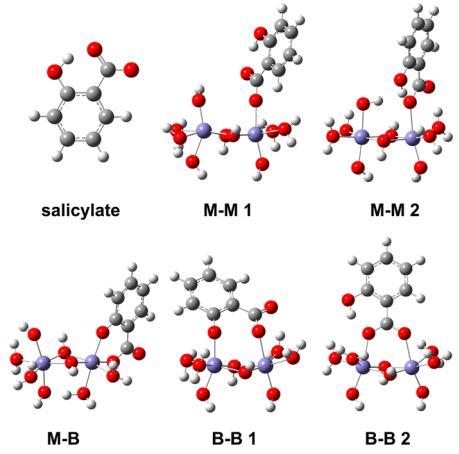


**Figure 4.** Optimized structures for salicylate, mononuclear monodentate (M-M), mononuclear bidentate (M-B), and binuclear bidentate (B-B) configurations. Explicit $H_2O$ molecules were not shown for clarity.

followed the Langmuir model $Q_e = KQ_{max}C_e/(KC_e + 1)$.[29] Here $Q_e$ is the equilibrium adsorbate concentration on goethite, $K$ is the adsorption constant, $Q_{max}$ is the maximum adsorption capacity, and $C_e$ is the equilibrium adsorbate concentration in solution. The maximum adsorption capacity $Q_{max}$ for salicylate


dx.doi.org/10.1021/jp4027578 | J. Phys. Chem. C 2013, 117, 10597−10606

Table 2. Calculated Peak Positions and Assignments for Mononuclear Mondentate (M-M), Mononuclear Bidentate (M-B), and Binuclear Bidentate (B-B) Structures

| pH 5[a] | pH 7[a] | pH 9[a] | M-M 1 | assignment | M-M 2 | assignment |
|---|---|---|---|---|---|---|
| 1149 | 1149 | 1149 | 1139 | $\delta$(CH) | 1142 | $\delta$(CH) |
| 1160 | 1160 | 1160 | 1175 | $\delta$(CH) | 1177 | $\delta$(CH) |
| 1246 | 1246 | 1246 | 1226 | $\nu$(ph−OH) | 1220 | $\nu$(ph−OH) |
| 1265 | 1266 | 1265 | 1307 | $\nu$(CC) | 1247 | $\delta$(ph−OH) |
| 1327 | 1327 | 1328 | 1319 | $\nu_s$(COO−) | 1299 | $\nu$(CC),$\delta$(ph−OH) |
| 1387 | 1387 | 1387 | 1375 | $\delta$(ph−OH), $\nu$(CC) | 1320 | $\nu_s$(COO−),$\nu$(CC) |
| 1462 | 1462 | 1462 | 1432 | $\nu$(CC) | 1376 | $\nu_{as}$(COO−) |
| 1477 | 1477 | 1476 | 1468 | $\nu$(CC) | 1427 | $\nu$(CC) |
| 1540 | 1538 | 1540 | 1500 | $\nu_{as}$(COO−) | 1468 | $\nu$(CC) |
| 1574 | 1574 | 1573 | 1567 | $\nu$(CC) | 1504 | $\nu$(CC),$\delta$(ph−OH) |
| 1610 | 1610 | 1609 | 1613 | $\nu$(CC) | 1559 | $\nu$(CC) |
| | | | | | 1563 | $\nu$(CC) |
| | | | | | 1586 | $\nu$(CC) |
| | | | | | 1620 | $\nu$(CC),$\delta$(ph−OH) |

| M-B | assignment | B-B 1 | assignment | B-B 2 | assignment |
|---|---|---|---|---|---|
| 1122 | $\delta$(CH) | 1157 | $\delta$(CH) | 1139 | $\delta$(CH) |
| 1163 | $\delta$(CH) | 1167 | $\delta$(CH) | 1167 | $\delta$(CH) |
| 1185 | $\nu$(ph-O) | 1222 | $\nu$(ph-O),$\nu$(CC) | 1213 | $\nu$(ph−OH) |
| 1219 | $\nu$(CC) | 1305 | $\nu$(ph-O),$\nu$(CC) | 1248 | $\nu$(ph−OH) |
| 1237 | $\nu$(CC) | 1344 | $\nu_s$(COO−) | 1314 | $\nu$(CC) |
| 1289 | $\nu_s$(COO−),$\nu$(CC) | 1404 | $\nu_{as}$(COO−),$\nu$(CC) | 1341 | $\nu_s$(COO−),$\delta$(ph−OH) |
| 1440 | $\nu$(CC) | 1448 | $\nu$(CC) | 1386 | $\nu_s$(COO−),$\delta$(ph−OH) |
| 1463 | $\nu$(CC) | 1455 | $\nu$(CC) | 1433 | $\nu$(CC) |
| 1531 | $\nu_{as}$(COO−),$\nu$(CC) | 1538 | $\nu$(CC) | 1468 | $\nu$(CC) |
| 1555 | $\nu$(CC) | 1581 | $\nu$(CC) | 1511 | $\nu_{as}$(COO−),$\delta$(ph−OH) |
| 1587 | $\nu$(CC) | | | 1564 | $\nu$(CC) |
| | | | | 1591 | $\nu$(CC) |
| | | | | 1621 | $\nu$(CC),$\delta$(ph−OH) |

[a]Observed frequencies of the interfacial spectra with 1 mM salicylate in 0.1 M NaCl. Peak assignments are based on theoretical calculations.

and catechol on goethite was calculated as 0.19 and 1.96 $\mu$mol/m$^2$, respectively. When it competed with equal molarity of catechol, salicylate adsorption decreased dramatically to nearly undetectable (Figure 1C). In contrast, the presence of salicylate had no detectable effect on the adsorption of catechol, as evidenced by the nearly unchanged $Q_{max}$, 1.95 $\mu$mol/m$^2$ (Figure 1D). The contrast adsorption behaviors of salicylate and catechol highlight the need for mechanistic study on the molecular level.

**2. ATR-FTIR Spectroscopy and DFT Calculation of Salicylate.** Salicylate (monoanion) is the predominant soluble species over a wide pH range 3−13 (Figure 2A). As predicted, the FTIR spectra of salicylate exhibited no perceptible difference at pH 5, 7, and 9 in 0.1 M NaCl solution (Figure 2B). Notably, a strong intramolecular hydrogen bond exists between the COO$^-$ group and the ortho ph−OH group.[7] This intramolecular hydrogen bond results in an anomalously high p$K_{a2}$ (13.7) of salicylate[7,30] and may lead to a unique surface structure.

The observed and DFT calculated frequencies as well as the peak assignments are listed in Table 1. In agreement with previous studies,[3,4,8,9] vibrations of $\nu$(CC) were resolved at about 1623, 1593, 1487, 1458, and 1303 cm$^{-1}$, $\nu_{as}$(COO$^-$) at 1570 cm$^{-1}$, $\nu$(ph−OH) at 1253 cm$^{-1}$, and $\delta$(CH) at 1159 and 1146 cm$^{-1}$. The band at 1387 cm$^{-1}$ was due to the combination of $\delta$(ph−OH) and $\nu$(CC). The band at ∼1341 cm$^{-1}$ was attributed to symmetric $\nu$ (COO$^-$) vibration.

**3. ATR-FTIR Spectra and DFT Calculations of Salicylate on Goethite.** The time-dependent spectra of interfacial species with 1 mM salicylate at pH 5, 7, and 9 in 0.1 M NaCl are illustrated in Figure 3. During adsorption, the peak position of the surface complex remained unchanged. Furthermore, nearly no difference in peak position and shape was observed for the adsorbed salicylate at pH 5, 7, and 9, indicating that the same interfacial configurations persist in the investigated pH range.

Compared with the spectra of aqueous salicylate (Figure 2B), the shape and position of the adsorbed salicylate changed significantly, suggesting the formation of inner-sphere surface complex.[21] The $\nu_{as}$(COO$^-$) in dissolved salicylate at 1570 cm$^{-1}$ shifted to ∼1540 cm$^{-1}$ upon adsorption, indicating that the COO$^-$ group is involved in the bond formation.[8] In addition, the $\nu$(ph−OH) for salicylate at 1253 cm$^{-1}$ decreased in frequency to 1246 cm$^{-1}$. This slight shift of 7 cm$^{-1}$ might be associated with a weakening of the intramolecular hydrogen bond to the ph−OH group rather than surface complexation.[5,7] Hence, the most plausible configuration would be in monodentate coordination involving an oxygen atom from the carboxylate.[5,11,12]

To justify the proposed surface complex, we employed the quantum chemical calculations for the adsorbed salicylate in five possible configurations including two M-M, one M-B, and two B-B structures (Figure 4). The M-M complexes interacted with the surface iron involving an oxygen atom of the carboxylate. In M-M 1, the intramolecular hydrogen bond remained to the oxygen atom in C═O as in the salicylate. In M-M 2, the phenolic group was hydrogen-bonded to the oxygen in the Fe−O−C group. The M-B structure may form


dx.doi.org/10.1021/jp4027578 | J. Phys. Chem. C 2013, 117, 10597−10606

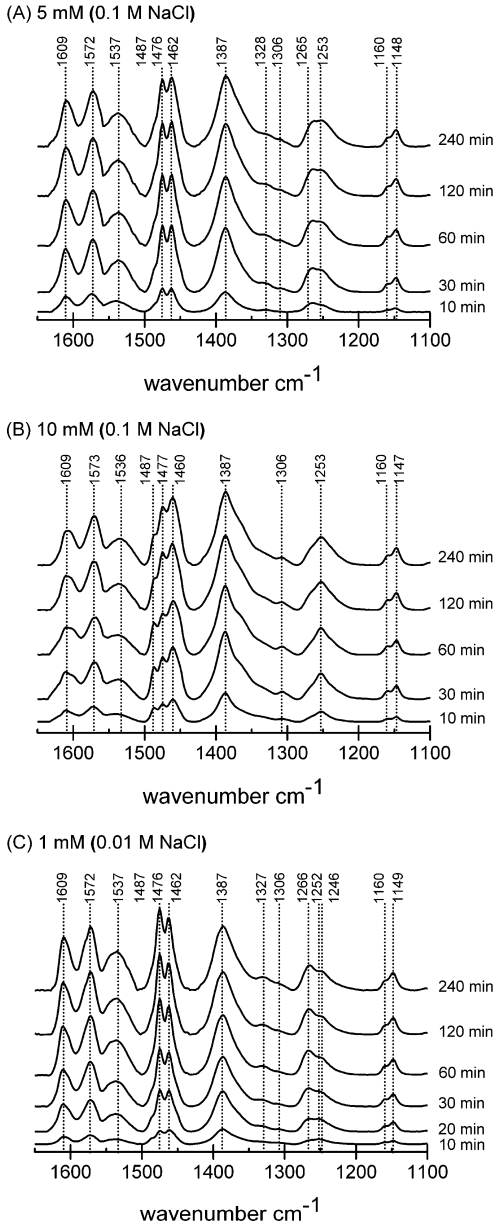


**Figure 5.** Time-dependent spectra of adsorbed species acquired with 5 mM (A) and 10 mM (B) salicylate at pH 5 in 0.1 M NaCl solution and 1 mM salicylate at pH 5 in 0.01 M NaCl (C).

when phenolic and carboxylate groups share one iron atom.[3,4,7] In the B-B 1 surface complex, both carboxylate and phenolic groups bonded to two iron atoms, while the two oxygen atoms in carboxylate group connect with two iron atoms in the B-B 2 configuration.

The plausible interfacial structure was scrutinized by the agreement between the observed IR vibrations and DFT calculations (Table 2).[5,21] The statistics analysis of correlations between experimental and calculated frequencies is included in the Supporting Information (SI). The results showed that the M-M 1 configuration fits the observed complex much better than the others. The formation of this M-M 1 surface complex has almost no effect on the geometry of the planar six-membered ring due to its strong intramolecular hydrogen bond.[11,31] Furthermore, this intramolecular hydrogen bond may, in turn, jeopardize the strength of the Fe−salicylate interactions, resulting in a relative weak inner-sphere complex. In agreement with our results, the same M-M 1 interfacial structure has been reported for salicylate adsorption on aluminum oxides.[5,11]

The shift in peak position was observed due to distortions of the salicylate structure upon adsorption on goethite surfaces.[21] The bands attributed to $\nu$(CC) vibration were shifted from about 1623, 1593, 1487, 1458, and 1303 $cm^{-1}$ in aqueous salicylate to 1610, 1574, 1477, 1462, and 1265 $cm^{-1}$ once adsorbed, respectively. The peak centered at 1387 $cm^{-1}$, corresponding to $\delta$(ph−OH) coupled to $\nu$(CC) modes, remained unchanged before and after adsorption. The band at ∼1341 $cm^{-1}$ corresponding to $\nu_s(COO^-)$ downshifted to ∼1327 $cm^{-1}$. The bands at 1160 and 1149 $cm^{-1}$ were due to $\delta$(CH) vibration.

**4. ATR-FTIR Spectra of Adsorbed Salicylate under the Effects of Concentration and Ionic Strength.** The time-dependent spectra with low salicylate concentration (10 $\mu$M, $I$ = 0.1 M NaCl) are shown in SI Figure S1. Frequencies of the dynamic spectra were the same as those collected with 1 mM salicylate solution, which further confirmed that the inner-sphere configuration was in the form of M-M 1 structure. No new surface complex was observed during the dynamic adsorption process.

The coexistence of M-M 1 inner-sphere and electrostatic outer-sphere complexes was observed with increased salicylate concentration as well as decreased ionic strength (Figure 5). The M-M 1 complex was evidenced by the similar peak positions and shape at about 1609, 1572, 1537, 1476, 1462, and 1387 $cm^{-1}$ as those in 1 mM salicylate surface complexes. The outer-sphere complex was identical to the free salicylate in solution, as demonstrated by the similar peak positions at 1487, 1306, and ∼1253 $cm^{-1}$ as those in the salicylate solution. The spectroscopic observations agreed well with our macroscopic pH edge results that the electrostatic outer-sphere surface complex formation should play a role in the adsorption of salicylate on goethite (Figure 1A). Notably, the strongly hydrogen-bonded surface species was almost unlikely for the adsorbed salicylate. The strong intramolecular hydrogen bond in salicylate suppressed the possibility of intermolecular hydrogen bonding between salicylate and goethite surface.[32,33]

The inner-sphere surface complex formation was the main mechanism of the interfacial reactions because its spectroscopic intensities were much higher than those of the outer-sphere complex. The spectroscopic features of the outer-sphere complex could only be clearly resolved with extremely high salicylate concentrations, that is, 10 mM (Figure 5B). The difficulty in the formation of outer-sphere complexes in 0.1 M NaCl could be primarily attributed to the strong competition from chloride. The effect of chloride competition was also supported by the appearance of a small amount of outer-sphere complexes with 1 mM salicylate in 0.01 M NaCl (Figure 5C). However, the outer-sphere adsorption features could not be clearly resolved after 30 min due to the significant increase in the inner-sphere complex.

**5. ATR-FTIR Spectra of Competitive Adsorption between Salicylate and Catechol.** Figure 6 shows the time-dependent spectra of 1 mM salicylate and catechol coadsorption on goethite at pH 5, 7, and 9 in 0.1 M NaCl. The interfacial configurations were not changed under different pH, as evidenced by the similar peak positions in the pH range 5−9. The results of the binary system resolved the individual spectroscopic features of salicylate and catechol adsorbed on goethite. The frequencies at the end of adsorption process


dx.doi.org/10.1021/jp4027578 | J. Phys. Chem. C 2013, 117, 10597−10606

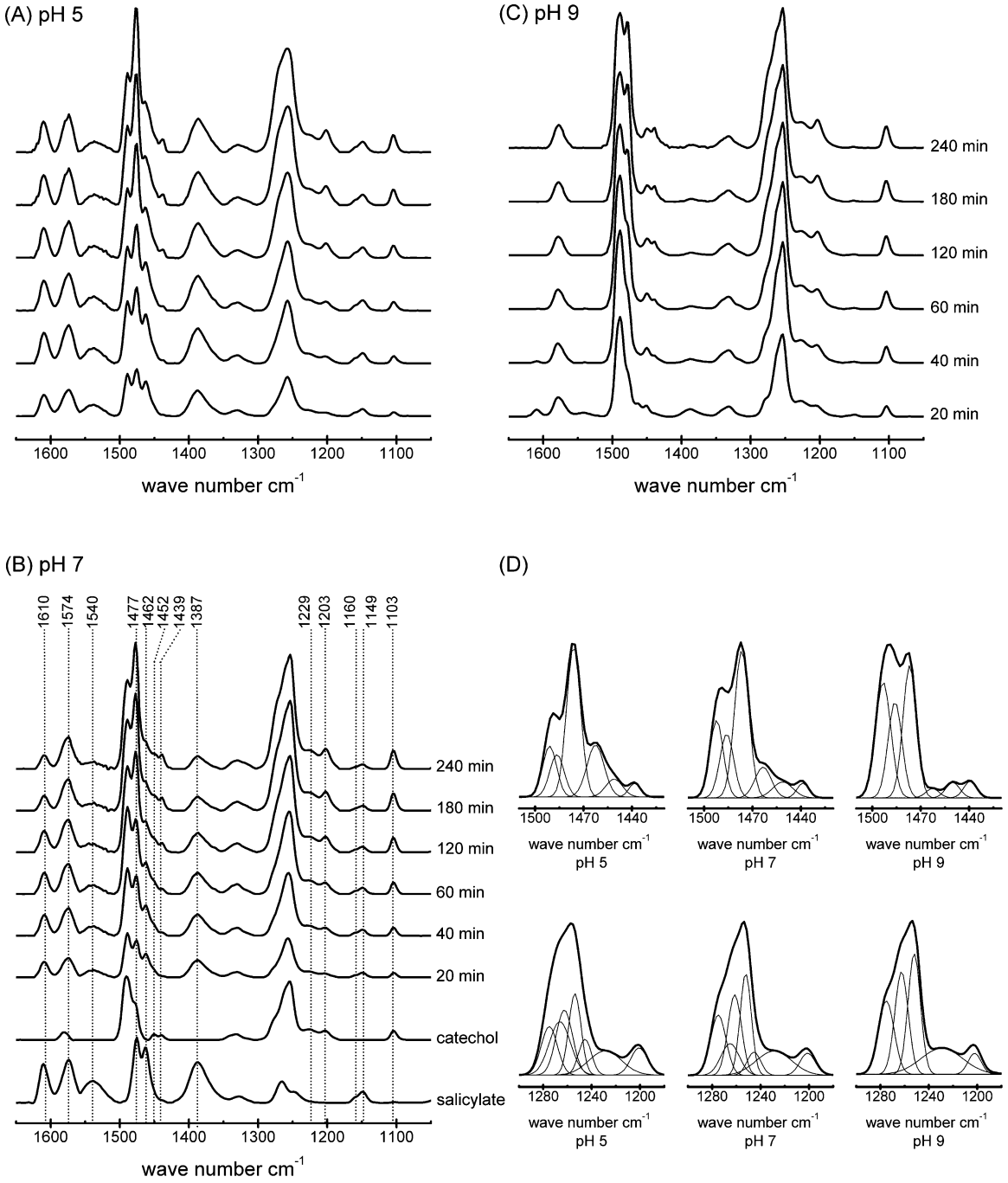


**Figure 6.** Time-dependent spectra of competitive adsorption acquired at pH 5 (A), pH 7 (B), and pH 9 (C) with 1 mM salicylate and catechol in 0.1 M NaCl solution. The spectra of adsorbed salicylate and catechol in the single adsorbate systems were also shown for comparison. (D) Curve-fitting results for spectra collected at 240 min under pH 5, 7, and 9 within the ranges of 1510−1420 $cm^{-1}$ (top) and 1300−1180 $cm^{-1}$ (bottom). Data of single catechol adsorption are from our previous study.[20]

could be divided into three configuration groups: M-M 1 for salicylate and M-M and B-B for catechol (Table 3). Curve-fitting results of the overlapped peaks in the 1510−1420 and 1300−1180 $cm^{-1}$ ranges are shown in Figure 6D as an example for pH 5, 7, and 9 collected at 240 min.

Variations in the peak intensity exhibited an uneven enhancement as a function of time, indicating the different adsorption rate for each surface complex. The dynamic adsorption process for each complex can be further explored using the change in their corresponding peak intensities (Figure 7).[34,35] Here the dynamic process of salicylate and catechol on goethite in single-adsorbate systems was also investigated for comparison. In this study, the 1387 $cm^{-1}$ peak was selected to monitor adsorption process of salicylate. The peaks of adsorbed catechol were heavily overlapped with those of adsorbed salicylate. Considering the stability in strength and shape, the peaks at 1229 and 1203 $cm^{-1}$ were chosen to monitor the adsorption process of catechol M-M and B-B structures, respectively.

In the absence of catechol, the adsorption of salicylate increased along with time, but the rate became slow after ~90 min without reaching equilibrium (Figure 7A). The difficulty in


dx.doi.org/10.1021/jp4027578 | J. Phys. Chem. C 2013, 117, 10597−10606

Table 3. Observed Peak Positions for Single Adsorbate, Competitive Adsorption I (Direct Competition) and II (Single Adsorbate First and then Competition) at 240 min[a]

| competition I | | | competition II | | single salicylate | single catechol* | |
|---|---|---|---|---|---|---|---|
| pH 5 | pH 7 | pH 9 | salicylate first | catechol first | M-M 1 | M-M | B-B |
| 1103 | 1103 | 1103 | 1104 | 1103 | | 1103 | 1103 |
| 1149 | 1149 | | 1150 | 1150 | 1149 | | |
| 1159 | 1160 | | 1159 | 1159 | 1160 | | |
| 1203 | 1203 | 1203 | 1203 | 1203 | | | 1203 |
| 1229 | 1229 | 1229 | 1229 | 1229 | | 1229 | |
| 1246 | 1246 | | 1245 | 1246 | 1246 | | |
| 1253 | 1253 | 1253 | 1253 | 1253 | | 1253 | |
| 1262 | 1263 | 1263 | 1262 | 1262 | | | 1263 |
| 1266 | 1267 | | 1266 | 1267 | 1266 | | |
| 1276 | 1275 | 1276 | 1276 | 1275 | | | 1276 |
| 1327 | | | | | 1327 | | |
| 1334 | 1334 | 1334 | 1333 | 1333 | | 1334 | |
| 1387 | 1387 | 1387 | 1387 | 1387 | 1387 | | |
| 1439 | 1439 | 1440 | 1438 | 1438 | | | 1439 |
| 1452 | 1452 | 1452 | 1451 | 1451 | | 1452 | |
| 1463 | 1462 | 1463 | 1462 | 1463 | 1462 | | |
| 1477 | 1477 | 1477 | 1477 | 1477 | 1477 | | 1477 |
| 1487 | 1487 | 1487 | 1487 | 1487 | | 1487 | |
| 1493 | 1494 | 1494 | 1493 | 1494 | | 1494 | |
| 1539 | 1540 | | 1539 | 1540 | 1538 | | |
| 1574 | 1574 | 1574 | 1573 | 1574 | 1574 | | |
| 1581 | 1580 | 1581 | 1580 | 1580 | | 1581 | |
| 1610 | 1610 | | 1609 | 1609 | 1610 | | |

[a]Observed frequencies for single salicylate and catechol adsorption were collected at pH 7. Data of single catechol adsorption are from our previous study.[20]

achieving adsorption equilibrium could be primarily attributable to its low surface coverage and weak inner-sphere affinity.

In contrast, salicylate exhibited different adsorption kinetics at pH 5, 7, and 9 in the presence of catechol (Figure 7B). At pH 5, the adsorption capacity increased with time and reached equilibrium rapidly within ∼60 min. The short equilibration time could be attributed to limited surface sites due to the competition by catechol. At pH 7, the surface complex achieved its highest adsorption at ∼60 min and then decreased and reached equilibrium at ∼180 min; at pH 9, the adsorption of salicylate decreased with time and reached equilibrium at ∼60 min. The decrease in intensity indicated that some adsorbed salicylate could be replaced by catechol. In addition, the rate of the replacement was much faster at pH 9 than that at pH 7. The discrepancy in replacement rate could be attributed to the different adsorption affinities of these two organic ligands under different pH conditions. Salicylate showed preferential adsorption under lower pH conditions, whereas catechol showed preferential adsorption under higher pH conditions (Figures 1 and 6).

The catechol B-B complexes exhibited similar adsorption kinetics at pH 5, 7, and 9 in the single adsorbate and competition systems; namely, the adsorption increased as a function of time without equilibrium within 240 min (Figure 7C,D). The consistent increase even after about 90 min was due to the attractive intermolecular interactions with the increased surface coverage that facilitate the stabilization of B-B surface complex.[20,36]

The introduction of salicylate enhanced the B-B type contribution to the overall catechol adsorption especially at pH 5, as evidenced by the increased ratio in peak intensities of 1203 to 1229 $cm^{-1}$ collected at 240 min, that is, 1.32 (pH 5), 1.10 (pH 7), and 1.09 (pH 9) in the competition system and 0.67 (pH 5), 0.86 (pH 7), and 0.86 (pH9) in the single catechol system (Figure 7C−F). The relative contributions of catechol M-M and B-B structures were associated with their adsorption affinity. The conversion from M-M to B-B structures at pH 9 in the single adsorbate system suggested the stronger bonding strength of B-B than M-M complex.[20] Moreover, the ph−OH group in the M-M configuration weakened the Fe-catechol bond.[28] As a result, the formation of catechol B-B complex was less affected by the competition of salicylate, which subsequently facilitated a higher catechol B-B complexation to the overall catechol adsorption. Notably, the stronger adsorption affinity of salicylate on goethite, the higher the B-B proportion in catechol adsorption would be. Accordingly, a substantial extent of the B-B complex was observed at low pH in the competition system.

The catechol M-M complex increased with time and then reached equilibrium in the competition system (Figure 7F). Interestingly, the equilibrium time at pH 5 and 7 was extended due to the salicylate competition from 90 min in the single system to ∼180 min in the binary system. At pH 9, the adsorption reached equilibrium rapidly within 90 min. However, the presence of salicylate inhibited the conversion of catechol from M-M to B-B structures compared with single catechol system (Figure 7E). The inhibition could be attributable to the decrease in relative catechol contents with M-M structure and steric effect from salicylate in the competition system.

The competition effect on the adsorption affinity of salicylate and catechol could be further confirmed by single adsorption first and then the competitive adsorption (Figure 8). After single salicylate/catechol adsorption, the interfacial spectra of


dx.doi.org/10.1021/jp4027578 | J. Phys. Chem. C 2013, 117, 10597−10606

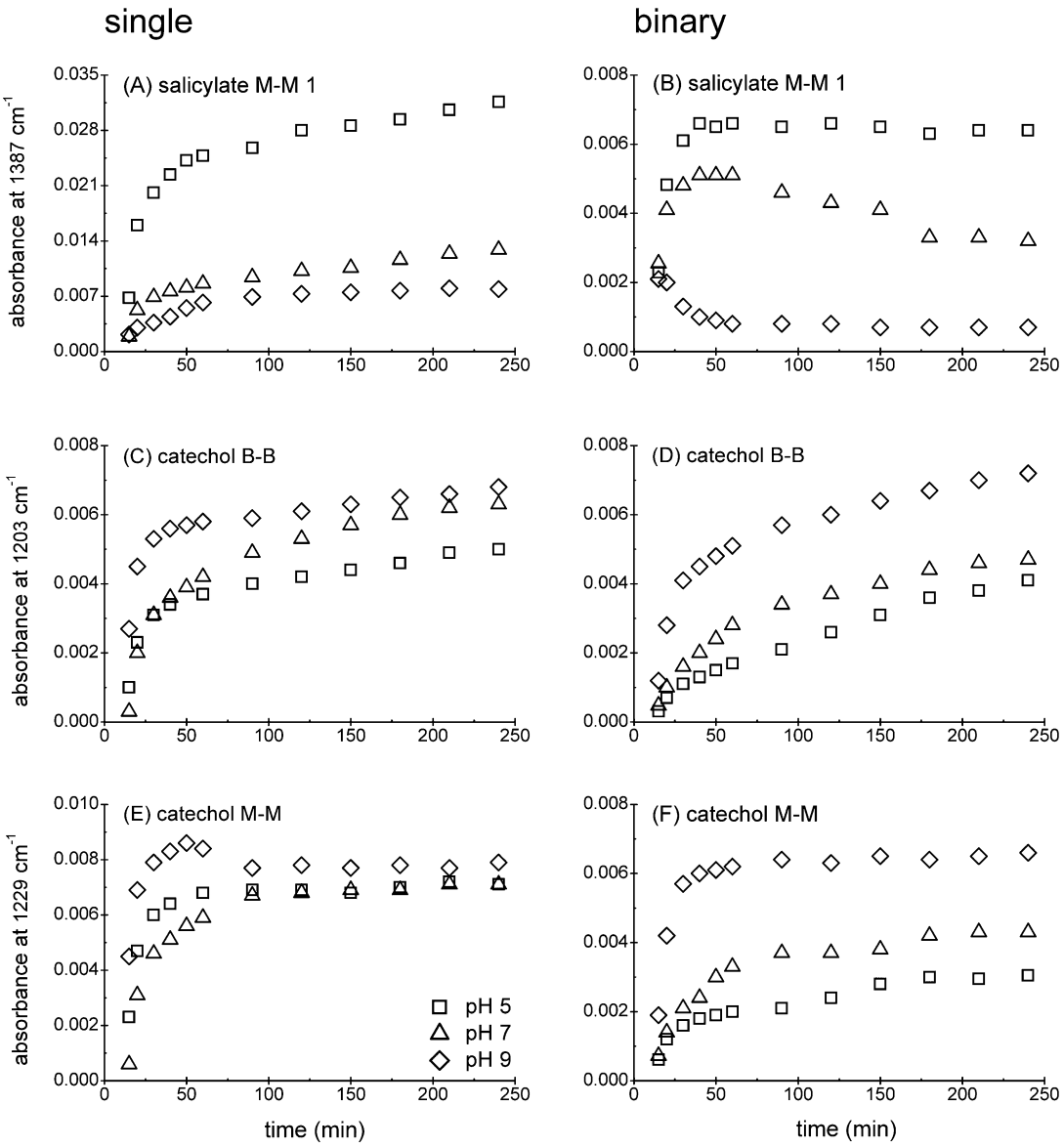


**Figure 7.** Dynamic variations in peak intensity of the bands at 1387, 1229, and 1203 $cm^{-1}$ at pH 5, 7, and 9 in 0.1 M NaCl solution with 1 mM salicylate and catechol in single and direct competition systems. Data of single catechol adsorption are from our previous study.[20]

the competition system also resolved the individual spectroscopic features of salicylate M-M 1 and catechol M-M and B-B configurations (Table 3). The frequencies at the end of adsorption process were almost the same as those in direct competitive adsorption with only 1 to 2 $cm^{-1}$ discrepancy.

Catechol exhibited stronger adsorption affinity than salicylate. In the presence of catechol, the adsorbed salicylate was replaced, and the adsorption reached equilibrium at ~210 min (Figure 9A). The replacement of adsorbed salicylate at pH 7 was also observed in the direct competitive adsorption system (Figure 7B). In contrast, the adsorption of catechol was slightly affected by the presence of salicylate (Figure 9B). The adsorption of catechol M-M complex reached equilibrium rapidly within 90 min. Compared with the direct competition system, the equilibration time was reduced (Figure 7F). The reason should be attributed to the decreased available surface sites for the competitive adsorption after single catechol adsorption. In line with the adsorption kinetics in the single catechol and direct competitive adsorption system, the B-B complex increased as a function of time without equilibrium within 240 min. The B-B type contribution to the overall catechol adsorption was also elevated due to the presence of salicylate, as evidenced by the increased ratio in peak intensities of 1203 to 1229 $cm^{-1}$ collected at 240 min, namely, 1.17 herein and 0.86 in the single catechol system.

The stronger adsorption affinity of catechol than salicylate was also justified in the competition after single-adsorbate adsorption. After single-salicylate adsorption, the catechol in the competitive adsorption exhibited similar adsorption kinetics as in the direct competition system (Figure 9A). After single-catechol adsorption, only minimal adsorption of salicylate was observed in the competition system (Figure 9B).

## ■ CONCLUSIONS

In this study, we investigated the dynamic adsorption process of salicylate on goethite under different pH, concentration, ionic strength, and competition with catechol. The FTIR spectra with 1 mM salicylate in 0.1 M NaCl resolved the M-M 1 type inner-sphere surface complex with the unbroken intramolecular


dx.doi.org/10.1021/jp4027578 | J. Phys. Chem. C 2013, 117, 10597−10606

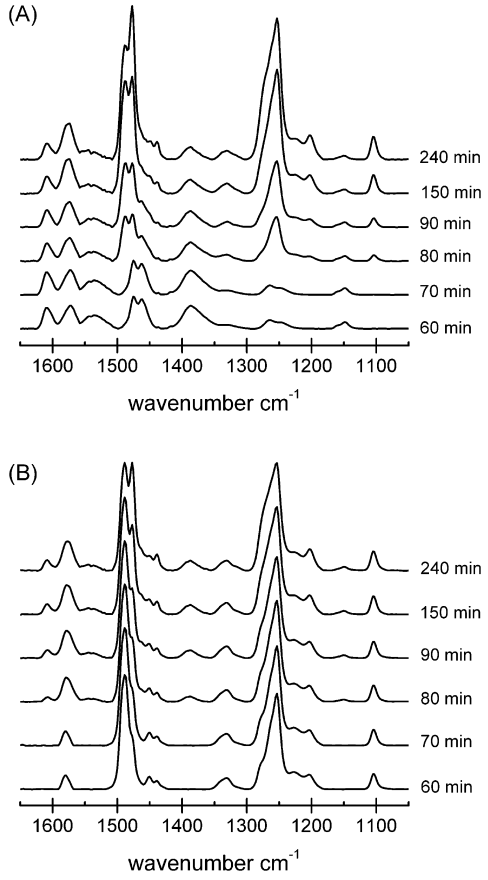


**Figure 8.** Time-dependent spectra of single adsorbate first and then the competitive adsorption acquired at pH 7 with 1 mM salicylate and catechol in 0.1 M NaCl solution.

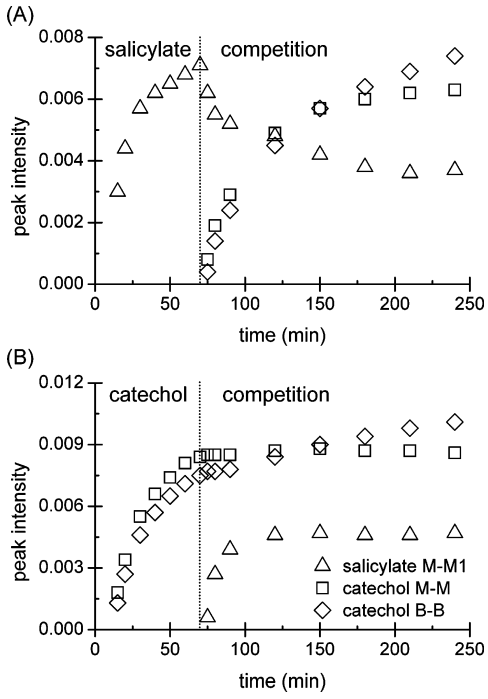


**Figure 9.** Dynamic variations in peak intensity of the bands at 1387, 1229, and 1203 $cm^{-1}$ at pH 7 in 0.1 M NaCl solution with 1 mM salicylate and catechol in single and then binary competition systems.

hydrogen bond as in the free salicylate. In line with the macroscopic adsorption results, the electrostatic outer-sphere complex was observed from the time-dependent spectra with increased salicylate concentration (5 and 10 mM) and decreased ionic strength (0.01 M NaCl). However, the outer-sphere adsorption played a minor role due to the strong competition from chloride.

In the competition system, the dynamic spectra with 1 mM salicylate and catechol in 0.1 M NaCl resolved individual features of surface salicylate and catechol complexes, and no new surface species have been detected. Catechol out-competed salicylate for adsorption, and thus the replacement of adsorbed salicylate by catechol occurred from pH 7 to 9. The introduction of salicylate elevated the B-B type complexation to the overall catechol adsorption. Furthermore, the presence of salicylate inhibited the conversion of catechol from M-M to B-B structures. The results provide insights into the surface complexes of salicylate and catechol on the molecular scale that can be used to describe and predict the behaviors of NOM in the environment.

## ■ ASSOCIATED CONTENT

### Supporting Information

Sensitivity analysis of the DFT calculation. Statistics analysis of correlations between experimental and DFT calculations. Dynamic spectra of 10 $\mu$M salicylate adsorbed on goethite at pH 5 in 0.1 M NaCl solution. Dissolution of goethite in batch adsorption and flow-cell ATR-FTIR experiments. This material is available free of charge via the Internet at http://pubs.acs.org.

## ■ AUTHOR INFORMATION

### Corresponding Author

*Tel: +86-10-62849523. Fax: +86-10-62849523. E-mail: cyjing@rcees.ac.cn.

### Notes

The authors declare no competing financial interest.

## ■ ACKNOWLEDGMENTS

The research is supported by the National Natural Science Foundation of China (41023005 and 20890112). The use of Deepcomp7000 in Computer Network Information Center of Chinese Academy of Sciences is acknowledged.

## ■ REFERENCES

(1) Thomas, H. Occurrence, Fate, and Removal of Pharmaceutical Residues in the Aquatic Environment: A Review of Recent Research Data. *Toxicol. Lett.* **2002**, *131*, 5−17.

(2) Borah, J. M.; Das, M. R.; Mahiuddin, S. Influence of Anions on the Adsorption Kinetics of Salicylate onto $\alpha$-Alumina in Aqueous Medium. *J. Colloid Interface Sci.* **2007**, *316*, 260−267.

(3) Yost, E. C.; Tejedor-Tejedor, M. I.; Anderson, M. A. In Situ CIR-FTIR Characterization of Salicylate Complexes at the Goethite/Aqueous Solution Interface. *Environ. Sci. Technol.* **1990**, *24*, 822−828.

(4) Rusch, B.; Hanna, K.; Humbert, B. Sorption and Transport of Salicylate in a Porous Heterogeneous Medium of Silica Quartz and Goethite. *Environ. Sci. Technol.* **2010**, *44*, 2447−2453.

(5) Trout, C. C.; Kubicki, J. D. UV Resonance Raman Spectra and Molecular Orbital Calculations of Salicylic and Phthalic Acids Complexed to $Al^{3+}$ in Solution and on Mineral Surfaces. *J. Phys. Chem. A* **2004**, *108*, 11580−11590.

(6) Axe, K.; Vejgården, M.; Persson, P. An ATR-FTIR Spectroscopic Study of the Competitive Adsorption between Oxalate and Malonate at the Water-Goethite Interface. *J. Colloid Interface Sci.* **2006**, *294*, 31−37.

(7) Biber, M. V.; Stumm, W. An in-Situ ATR-FTIR Study: The Surface Coordination of Salicylic Acid on Aluminum and Iron(III) Oxides. *Environ. Sci. Technol.* **1994**, *28*, 763−768.
(8) Tunesi, S.; Anderson, M. A. Surface Effects in Photochemistry: An in Situ Cylindrical Internal Reflection-Fourier Transform Infrared Investigation of the Effect of Ring Substituents on Chemisorption onto Titania Ceramic Membranes. *Langmuir* **1992**, *8*, 487−495.
(9) Dobson, K. D.; McQuillan, A. J. In Situ Infrared Spectroscopic Analysis of the Adsorption of Aromatic Carboxylic Acids to $TiO_2$, $ZrO_2$, $Al_2O_3$, and $Ta_2O_5$ from Aqueous Solutions. *Spectrochim. Acta, Part A* **2000**, *56*, 557−565.
(10) Janković, I. A.; Šaponjić, Z. V.; Čomor, M. I.; Nedeljković, J. M. Surface Modification of Colloidal $TiO_2$ Nanoparticles with Bidentate Benzene Derivatives. *J. Phys. Chem. C* **2009**, *113*, 12645−12652.
(11) Das, M. R.; Sahu, O. P.; Borthakur, P. C.; Mahiuddin, S. Kinetics and Adsorption Behaviour of Salicylate on $\alpha$-Alumina in Aqueous Medium. *Colloids Surf., A* **2004**, *237*, 23−31.
(12) Molis, E.; Barrès, O.; Marchand, H.; Sauzéat, E.; Humbert, B.; Thomas, F. Initial Steps of Ligand-Promoted Dissolution of Gibbsite. *Colloids Surf., A* **2000**, *163*, 283−292.
(13) Lindegren, M.; Persson, P. Competitive Adsorption Involving Phosphate and Benzenecarboxylic Acids on Goethite—Effects of Molecular Structures. *J. Colloid Interface Sci.* **2010**, *343*, 263−270.
(14) Thomas, J. E.; Kelley, M. J. A Study of Competitive Adsorption of Organic Molecules onto Mineral Oxides Using DRIFTS. *J. Colloid Interface Sci.* **2010**, *342*, 474−478.
(15) Norén, K.; Persson, P. Co-Adsorption of Ga(III) and EDTA at the Water−$\alpha$-FeOOH Interface: Spectroscopic Evidence of the Formation of Ternary Surface Complexes. *J. Phys. Chem. C* **2010**, *114*, 16547−16555.
(16) Simanova, A. A.; Loring, J. S.; Persson, P. Formation of Ternary Metal-Oxalate Surface Complexes on $\alpha$-FeOOH Particles. *J. Phys. Chem. C* **2011**, *115*, 21191−21198.
(17) Xing, B.; Pignatello, J. J. Competitive Sorption between 1,3-Dichlorobenzene or 2,4-Dichlorophenol and Natural Aromatic Acids in Soil Organic Matter. *Environ. Sci. Technol.* **1998**, *32*, 614−619.
(18) Ding, X.; Song, X.; Boily, J.-F. Identification of Fluoride and Phosphate Binding Sites at FeOOH Surfaces. *J. Phys. Chem. C* **2012**, *116*, 21939−21947.
(19) Aquino, A. J. A.; Tunega, D.; Haberhauer, G.; Gerzabek, M. H.; Lischka, H. Quantum Chemical Adsorption Studies on the (110) Surface of the Mineral Goethite. *J. Phys. Chem. C* **2007**, *111*, 877−885.
(20) Yang, Y.; Yan, W.; Jing, C. Dynamic Adsorption of Catechol at the Goethite/Aqueous Solution Interface: A Molecular-Scale Study. *Langmuir* **2012**, *28*, 14588−14597.
(21) Ha, J.; Hyun Yoon, T.; Wang, Y.; Musgrave, C. B.; Brown, J. G. E. Adsorption of Organic Matter at Mineral/Water Interfaces: 7. ATR-FTIR and Quantum Chemical Study of Lactate Interactions with Hematite Nanoparticles. *Langmuir* **2008**, *24*, 6683−6692.
(22) Frisch, M. J.; Trucks, G. W.; Schlegel, H. B.; Scuseria, G. E.; Robb, M. A.; Cheeseman, J. R.; Scalmani, G.; Barone, V.; Mennucci, B.; Petersson, G. A. et al. *Gaussian 09*, revision B.01; Gaussian, Inc.: Wallingford, CT, 2010.
(23) *NIST Computational Chemistry Comparison and Benchmark Database*; NIST Standard Reference Database Number 101, Release 15b; Johnson R. D., III, Ed.; August 2011. http://cccbdb.nist.gov/.
(24) He, G.; Zhang, M.; Pan, G. Influence of pH on Initial Concentration Effect of Arsenate Adsorption on $TiO_2$ Surfaces: Thermodynamic, DFT, and EXAFS Interpretations. *J. Phys. Chem. C* **2009**, *113*, 21679−21686.
(25) Kwon, K. D.; Kubicki, J. D. Molecular Orbital Theory Study on Surface Complex Structures of Phosphates to Iron Hydroxides: Calculation of Vibrational Frequencies and Adsorption Energies. *Langmuir* **2004**, *20*, 9249−9254.
(26) Hedberg, J.; Henriquez, J.; Baldelli, S.; Johnson, C. M.; Leygraf, C. Initial Atmospheric Corrosion of Zinc Exposed to Formic Acid, Investigated by in Situ Vibrational Sum Frequency Spectroscopy and Density Functional Theory Calculations. *J. Phys. Chem. C* **2008**, *113*, 2088−2095.
(27) Sun, H.; Lee, H. H.; Blakey, I.; Dargaville, B.; Chirila, T. V.; Whittaker, A. K.; Smith, S. C. Multiple Hydrogen-Bonded Complexes Based on 2-Ureido-4[1H]-pyrimidinone: A Theoretical Study. *J. Phys. Chem. B* **2011**, *115*, 11053−11062.
(28) Evanko, C. R.; Dzombak, D. A. Influence of Structural Features on Sorption of NOM-Analogue Organic Acids to Goethite. *Environ. Sci. Technol.* **1998**, *32*, 2846−2855.
(29) Liu, F.-F.; Wang, S.-G.; Fan, J.-L.; Ma, G.-H. Adsorption of Natural Organic Matter Surrogates from Aqueous Solution by Multiwalled Carbon Nanotubes. *J. Phys. Chem. C* **2012**, *116*, 25783−25789.
(30) Humbert, B.; Alnot, M.; Quilès, F. Infrared and Raman Spectroscopical Studies of Salicylic and Salicylate Derivatives in Aqueous Solution. *Spectrochim. Acta, Part A* **1998**, *54*, 465−476.
(31) Mardis, K. L.; Brune, B. J.; Vishwanath, P.; Giorgis, B.; Payne, G. F.; Gilson, M. K. Intramolecular versus Intermolecular Hydrogen Bonding in the Adsorption of Aromatic Alcohols onto an Acrylic Ester Sorbent. *J. Phys. Chem. B* **2000**, *104*, 4735−4744.
(32) Brune, B. J.; Koehler, J. A.; Smith, P. J.; Payne, G. F. Correlation between Adsorption and Small Molecule Hydrogen Bonding. *Langmuir* **1999**, *15*, 3987−3992.
(33) Glemza, A. J.; Mardis, K. L.; Chaudhry, A. A.; Gilson, M. K.; Payne, G. F. Competition between Intra- and Intermolecular Hydrogen Bonding: Effect on para/ortho Adsorptive Selectivity for Substituted Phenols. *Ind. Eng. Chem. Res.* **2000**, *39*, 463−472.
(34) Chiem, L. T.; Huynh, L.; Ralston, J.; Beattie, D. A. An in Situ ATR−FTIR Study of Polyacrylamide Adsorption at the Talc Surface. *J. Colloid Interface Sci.* **2006**, *297*, 54−61.
(35) Beaussart, A.; Petrone, L.; Mierczynska-Vasilev, A.; McQuillan, A. J.; Beattie, D. A. In Situ ATR FTIR Study of Dextrin Adsorption on Anatase $TiO_2$. *Langmuir* **2012**, *28*, 4233−4240.
(36) Liu, L.-M.; Li, S.-C.; Cheng, H.; Diebold, U.; Selloni, A. Growth and Organization of an Organic Molecular Monolayer on $TiO_2$: Catechol on Anatase (101). *J. Am. Chem. Soc.* **2011**, *133*, 7816−7823.